

# Fidelity threshold for long-range entanglement in quantum networks

Sébastien Perseguers\*

Max-Planck-Institut für Quantenoptik, Hans-Kopfermann-Strasse 1, D-85748 Garching, Germany

(Dated: November 6, 2018)

A strategy to generate long-range entanglement in noisy quantum networks is presented. We consider a cubic lattice whose bonds are partially entangled mixed states of two qubits, and where quantum operations can be applied perfectly at the nodes. In contrast to protocols designed for one- or two-dimensional regular lattices, we find that entanglement can be created between arbitrarily distant qubits if the fidelity of the bonds is higher than a critical value, independent of the system size. Therefore, we show that a constant overhead of local resources, together with connections of finite fidelity, is sufficient to achieve long-distance quantum communication in noisy networks.

PACS numbers: 03.67.Hk, 03.67.Pp

## I. INTRODUCTION

Quantum networks play a major role in quantum information processing [1], as in distributed quantum computation or in quantum communication [2, 3]. In fact they naturally describe the situation where neighboring stations (nodes) share partially entangled states of qubits (noisy links). One of the main tasks of quantum information processing is then to design protocols that establish entanglement between any pair of nodes, regardless of their distance in the network.

Quantum repeaters offer a first solution to this question: one can efficiently entangle the two extremities of a one-dimensional lattice of size  $N$  by iterating purification steps and entanglement swappings [4, 5]. This strategy needs  $\mathcal{O}(\log N)$  qubits at each node and runs in a time that scales as  $\mathcal{O}(\text{poly } N)$ . Though being very promising, their realization raises some technical problems, such as the need for reliable quantum memories [6], or the difficulty in manipulating many qubits per station. The latter difficulty is surmounted in [7], where only a constant number of qubits is required at each station. Various protocols improving the rate of long-distance quantum communication have been proposed over the past few years (see [8] and references therein), but either their time scaling remains polynomial in  $N$  or they are based on rather complicated quantum error correcting codes [9].

Motivated by the discovery of powerful protocols in the case of two-dimensional pure-state networks [10], another scheme for entanglement generation over long distance in noisy networks was presented in [11]. It exploits the higher connectivity of the nodes to gain information on the errors introduced by the noisy teleportations. This leads to a “one-shot” protocol where elementary entangled pairs are used only once, which thus relaxes the requirement of efficient quantum memories; see [12] for the latest quantum communication protocol in square lattices. However, the overhead of local resources in these two-dimensional systems still slightly increases with  $N$  (logarithmic dependence).

In this work, we show that entanglement generation

over arbitrarily long distance and using the minimum amount of resources (constant number of qubits per node and quantum operations executed in a constant time) can be achieved in three-dimensional lattices. For this result to hold, the fidelity  $F$  of the elementary links has to be larger than a threshold  $F^*$ . We first provide an analytical upper bound on this value and then present a numerical estimate based on Monte Carlo simulations.

## II. DESCRIPTION OF THE MODEL

We consider a cubic network that consists of  $N^3$  vertices, each of them possessing six qubits (except the ones lying on the sides of the cube), on which arbitrary quantum operations can be applied perfectly. Nearest neighbors share one partially entangled state of the form

$$\rho = (1 - \varepsilon)^2 |\Phi^+\rangle\langle\Phi^+| + \varepsilon(1 - \varepsilon) |\Psi^+\rangle\langle\Psi^+| + \varepsilon(1 - \varepsilon) |\Phi^-\rangle\langle\Phi^-| + \varepsilon^2 |\Psi^-\rangle\langle\Psi^-|. \quad (1)$$

Such a state can be realized as follows: a station prepares locally a maximally entangled pair of qubits, and sends one of them to a neighbor. In the quantum channel, the traveling qubit undergoes random and independent bit-flip and phase errors with probability  $0 < \varepsilon < 0.5$ . This channel describes a specific physical process, but the generality of  $\rho$  is in reality complete. In fact, we show in App. A that any entangled state of two qubits can be brought to this form by local quantum operations and classical communication. Finally, all classical processes (communication and computation) are assumed to take much less time than any quantum operation.

*Remark 1.* Physical implementations of three-dimensional lattices have been proposed in the context of quantum information processing and distributed quantum computation [13, 14]. For practical reasons, however, it may be advantageous to realize the proposed construction in two dimensions, using a “slice-by-slice” generation similar to the techniques developed in [15]. In that case note that the time required to run the protocol scales linearly with  $N$ .

*Remark 2.* Recently, ideas of percolation theory have been applied successfully to the case of mixed states of

---

\*Electronic address: sebastien.perseguers@mpq.mpg.de



FIG. 1: (Color online) Non-local control phase on two qubits  $A$  and  $B$ , with the help of a Bell pair  $|\Phi^+\rangle_{A'B'}$ .

rank two [16]. In addition to the fact that the techniques are very different, our study is not restricted to amplitude damping channels, but considers full-rank mixed states which are robust against any small perturbations. In fact our protocol still works if dependent bit-flip and phase errors are present in the connections.

### III. A MAPPING TO NOISY CLUSTER STATES

It was shown in [11] how to create and propagate a large Greenberger-Horne-Zeilinger (GHZ) state in a noisy square lattice. This state is robust against bit flips if their rate is not too high but is very fragile against phase errors. Any of them indeed destroys the coherence of the GHZ state. Therefore, an encoding of the qubits is required, which leads to a logarithmic scaling of the physical resources per node. Since we are looking for a fidelity threshold, we want to create a large state that has the ability to correct both bit-flip and phase errors. Cluster states thus arise as a natural choice. In fact they have been shown to possess an intrinsic capability of error correction, so that long-range entanglement between two faces of an infinite noisy cubic cluster state is indeed possible [17]. Our protocol is based on this construction, with two radical differences, however: first, the settings are distinct, and second, we allow only local quantum operations on *all* the nodes.

A cluster state, which is an instance of graph states, can be constructed by inserting a qubit in the state  $|+\rangle$  at each vertex of the graph and by applying a control phase between all neighboring pairs [18]. In our setting we cannot perform these control phases since they are non-local quantum operations, but we can add an ancillary qubit and perform joint measurements at each node such that the resulting state is a cluster state. This method has been described in [19] in the case of perfect links, which can be interpreted as the virtual components of a large valence-bond state, and has been generalized to imperfect connections in [17]. Nevertheless, let us describe here an explicit (and slightly different) construction, mainly for completeness sake but also for relating precisely the error rate in the quantum networks with the one in the noisy cluster state.

At each node, we add a qubit  $|+\rangle$  and use the noisy links  $\rho$  to indirectly perform the control phases. Let us first describe how this is achieved if all connections are perfect, i.e. their qubits are in the state  $|\Phi^+\rangle$ . We consider two nodes of the lattice, with two qubits  $A$  and  $B$  in the states  $|a\rangle = a_0|0\rangle + a_1|1\rangle$  and  $|b\rangle = b_0|0\rangle + b_1|1\rangle$ , and a connection  $|\Phi^+\rangle$  between two qubits  $A'$  and  $B'$ ,

see Fig. 1. We start by applying, on the qubits of the first node, the measurement operators

$$\begin{aligned} \mathcal{A}_0 &= |0\rangle_A \langle 00|_{AA'} + |1\rangle_A \langle 11|_{AA'}, \\ \mathcal{A}_1 &= |0\rangle_A \langle 01|_{AA'} + |1\rangle_A \langle 10|_{AA'}, \end{aligned} \quad (2)$$

with  $\sum_{i=0}^1 \mathcal{A}_i^\dagger \mathcal{A}_i = \mathbb{1}_4$ , which are followed by a bit flip  $X$  on  $B'$  if the outcome is  $\mathcal{A}_1$ . The resulting state on  $A$  and  $B'$  reads  $a_0|00\rangle + a_1|11\rangle$ . We then apply the second measurement

$$\begin{aligned} \mathcal{B}_0 &= |0\rangle_B \langle +0|_{B'B} + |1\rangle_B \langle -1|_{B'B}, \\ \mathcal{B}_1 &= |0\rangle_B \langle -0|_{B'B} + |1\rangle_B \langle +1|_{B'B}, \end{aligned} \quad (3)$$

followed by the matrix  $Z$  on  $A$  if we get  $\mathcal{B}_1$  as outcome. Finally,  $A$  and  $B$  are left in the (entangled) state

$$|C_{ab}\rangle = a_0 b_0 |00\rangle + a_0 b_1 |01\rangle + a_1 b_0 |10\rangle - a_1 b_1 |11\rangle,$$

which is the result of a control phase between  $|a\rangle$  and  $|b\rangle$ . Clearly, if  $|a\rangle = |b\rangle = |+\rangle$ , the state  $|C_{ab}\rangle$  is the cluster state on two qubits. Now, let us determine which errors occur if we blindly perform the very same operations but using another Bell state. It is straightforward to compute the results of these operations if one uses  $|\Psi^+\rangle$ ,  $|\Phi^-\rangle$ , or  $|\Psi^-\rangle$  for the connections: one gets  $\mathbb{1}_2 \otimes Z |C_{ab}\rangle$ ,  $Z \otimes \mathbb{1}_2 |C_{ab}\rangle$ , or  $Z \otimes Z |C_{ab}\rangle$ , respectively. Since the matrices  $Z$  commute with the control phases, it follows that errors do not propagate while constructing a (noisy) cluster state  $\rho_{CS}$  from the cubic quantum network. Moreover, because of the specific choice of coefficients in Eq. (1),  $Z$  errors appear independently at the nodes. Since a node of the lattice has degree six at most, and two  $Z$  errors cancel each other, the vertices of the resulting cluster state suffer an error with a probability at most equal to

$$p = \sum_{i=0}^2 \binom{6}{2i+1} \varepsilon^{2i+1} (1-\varepsilon)^{5-2i}. \quad (4)$$

This expression reduces to  $p \approx 6\varepsilon$  in the regime of small error rates. Therefore, we are exactly in the setting of [17], where thermal fluctuations in the cluster state induce independent local  $Z$  errors with rate  $p$ .

### IV. LONG-RANGE ENTANGLEMENT IN NOISY CLUSTER STATES

In this section, we mainly follow the construction and the notation proposed in [17], namely, the measurement of the qubits of  $\rho_{CS}$  according to a specific pattern of local bases. The outcomes of the measurements are random, but the choice of the bases establishes some parity constraints on them. Any violation of these constraints indicates an error, and a classical processing of all collected ‘‘syndromes’’ allows one to reliably identify the typical errors. This correction works perfectly for small error rates, but it breaks down at  $p_c \approx 3.3\%$  [20]. The difference between the present method and that given in

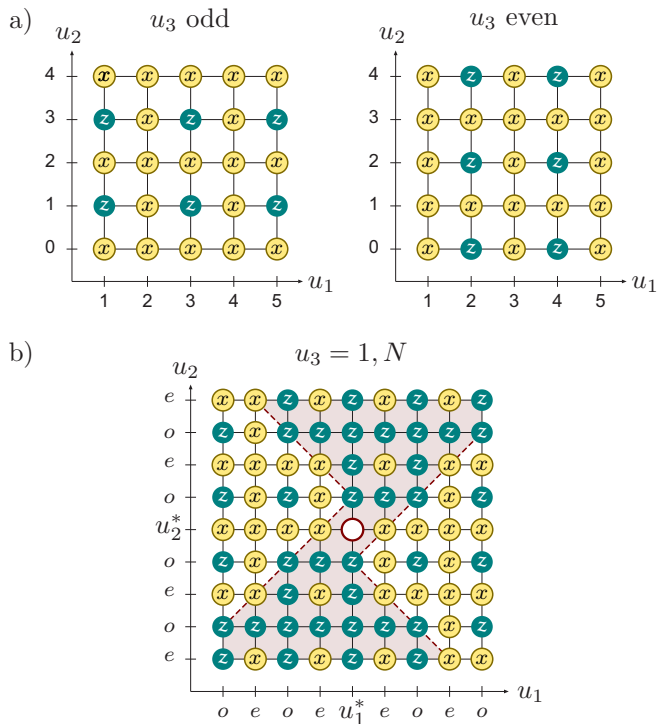


FIG. 2: (Color online) a) Bases in which qubits in the bulk of the cluster state are measured. b) Slightly different measurement pattern for the faces  $\mathcal{L}$  and  $\mathcal{R}$ : the central qubit is kept intact, and all qubits that lie in the shaded area are measured in the  $Z$  basis, except the ones with coordinates  $(e, e, 1)$  or  $(e, e, N)$ , which are measured in the  $X$  basis.

[17] is that no non-local quantum operation is allowed. This obliges us to design a more elaborated error correction, leading to a different type of long-distance entanglement. In fact we are not going to create a pure and perfect Bell pair of logical qubits, but rather a mixture of two entangled physical qubits.

### A. Measurement pattern and long-distance quantum correlations

Let us define a finite three-dimensional cluster state on the cube

$$\mathcal{C} = \{u = (u_1, u_2, u_3) : 1 \leq u_1, u_2 + 1, u_3 \leq N\},$$

and select two qubits  $A$  and  $B$  centered in two opposite faces  $\mathcal{L}$  and  $\mathcal{R}$ . The coordinates of these qubits are  $(u_1^*, u_2^*, 1)$  and  $(u_1^*, u_2^*, N)$ , with  $u_1^* = u_2^* + 1 = (N + 1)/2$ . For a reason that will soon become clear, we consider lattices of size  $N \equiv 1 \pmod{4}$ , so that  $u_1^*$  is odd and  $u_2^*$  even. Let us also introduce two disjoint sublattices  $T_o$  and  $T_e$  with double spacing, where  $o$  and  $e$  stand for odd and even. Their vertices are

$$\begin{aligned} V(T_o) &= \{u = (o, o, o)\} \subset \mathcal{C}, \\ V(T_e) &= \{u = (e, e, e)\} \subset \mathcal{C}, \end{aligned}$$

and their edges are given by the sets

$$\begin{aligned} E(T_o) &= \{u = (o, o, e), (o, e, o), (e, o, o)\} \subset \mathcal{C}, \\ E(T_e) &= \{u = (e, e, o), (e, o, e), (o, e, e)\} \subset \mathcal{C}. \end{aligned}$$

We also define the planes

$$\begin{aligned} T_X^{(u_2)} &= \{u = (o, u_2, o)\} \subset T_o, \\ T_Z^{(u_1)} &= \{u = (u_1, e, e)\} \subset T_e, \end{aligned}$$

and denote by  $T_X^*$  and  $T_Z^*$  the planes that contain  $A$  and  $B$ . These planes will be used to derive the Bell correlations of the future long-distance entangled state  $|\psi\rangle_{AB}$  (we first consider that no error occurs, and then extend the results to noisy cluster states). Qubits that belong to the vertices of  $T_o$  and  $T_e$  are measured in the  $Z$  basis, while all other qubits are measured in the  $X$  basis. There are, however, some exceptions in  $\mathcal{L}$  and  $\mathcal{R}$  (see Fig. 2): First, the central qubit is not measured, since it will be part of the long-distance entangled state. Second, qubits with coordinates  $u_1 = u_1^*$  are measured in the  $Z$  basis in order to create the right quantum correlations, as explained in the following paragraph. Finally, we measure in the  $Z$  basis all qubits whose first two coordinates are  $(e, o)$  or  $(o, e)$  and which lie in the shaded areas; these outcomes will be important for the error correction.

To compute the effect of the measurements on the quantum correlations between  $A$  and  $B$ , we use the fact that a perfect cluster state  $|C\rangle$  obeys the eigenvalue equation  $K_u |C\rangle = |C\rangle$  for all  $u \in \mathcal{C}$ , where  $K_u$  is the stabilizer

$$K_u = X_u \prod_{v \in \mathcal{N}(u)} Z_v, \quad (5)$$

with  $\mathcal{N}(u)$  the neighborhood of  $u$ . If we let the products of stabilizers  $\prod_{u \in T_X^*} K_u$  and  $\prod_{u \in T_Z^*} K_u$  act on the cluster state, we find that  $A$  and  $B$  are indeed maximally entangled:

$$\begin{aligned} X_A X_B |\psi\rangle_{AB} &= \lambda_X |\psi\rangle_{AB}, \\ Z_A Z_B |\psi\rangle_{AB} &= \lambda_Z |\psi\rangle_{AB}, \end{aligned} \quad (6)$$

with  $\lambda_X, \lambda_Z \in \{-1, +1\}$ . The eigenvalues  $\lambda_{X,Z}$  are calculated from the measurement outcomes  $x$  and  $z$ :

$$\begin{aligned} \lambda_X &= \prod_{u \in \Omega_X^{(z)}} z_u \prod_{u \in \Omega_X^{(x)}} x_u, \\ \lambda_Z &= \prod_{u \in \Omega_Z^{(z)}} z_u \prod_{u \in \Omega_Z^{(x)}} x_u, \end{aligned} \quad (7)$$

where  $\Omega_X^{(x)} = T_X^* \setminus \{A, B\}$ ,  $\Omega_Z^{(x)} = T_Z^*$ ,  $\Omega_X^{(z)} = T_X^{(u_2^*+1)} \cup T_X^{(u_2^*-1)}$ , and  $\Omega_Z^{(z)} = T_Z^{(u_1^*+1)} \cup T_Z^{(u_1^*-1)} \cup \{(u_1^*, e, 1), (u_1^*, e, N)\} \setminus \{A, B\}$ .

### B. Error correction

As already mentioned, measurement outcomes are random but not independent. It is thus possible to assign

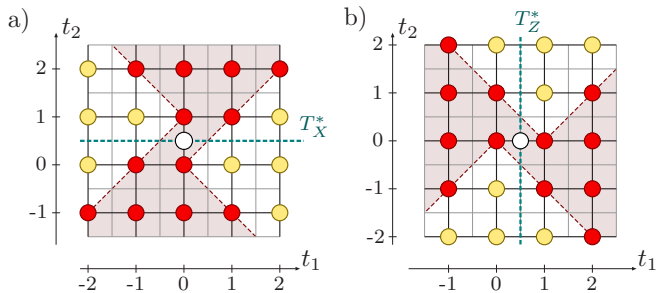


FIG. 3: (Color online) a) In red (dark disks), missing syndromes on the vertices of  $T_o$ , in  $\mathcal{L}$  and  $\mathcal{R}$ , corresponding to the measurement pattern depicted in Fig. 2c. Rough faces lie on the top and the bottom of this lattice. A new coordinate system  $(t_1, t_2, t_3)$  is introduced for the vertices of the sublattice. b) Same considerations for the  $Z$  correlation: the missing syndromes create additional rough surfaces in  $T_e$ .

to most vertices  $u_i \in T_i$ , with  $i = o$  or  $e$ , the parity syndrome

$$s(u_i) = \prod_{v \in \mathcal{N}(u_i)} x_v \prod_{w \in \mathcal{N}_i(u_i)} z_w, \quad (8)$$

where  $\mathcal{N}_i(u_i)$  designates the neighborhood of  $u_i$  in  $T_i$ . Since this equation arises from a product of stabilizers,  $\prod_{v \in \mathcal{N}_i(u_i)} K_v$ , we have that  $s(u_i) = 1$  if no error occurs on the qubits of  $\mathcal{N}_i(u_i)$ . The key point of the construction is that a  $Z$  error on any edge of  $T_i$  changes the sign of the two syndromes at its extremities. This is due to the fact that  $Z$  errors do not commute with  $X$  measurements, while outcomes  $z$  are not affected by them. The sublattices are treated separately, but in a similar way. We refer the reader to [17, 21] for a detailed discussion of the error recovery or to App. B for the basics to understand our protocol. In contrast with [17], and apart from the rough faces present in any surface code, we also suffer a lack of syndrome information in  $\mathcal{L}$  and  $\mathcal{R}$ . We cannot have a perfect and complete syndrome pattern for both  $T_o$  and  $T_e$  in these faces; for this to happen one should be able to measure both  $x$  and  $z$  eigenvalues of the concerned qubits, which is impossible, or apply non-local quantum operations, which we do not allow. Actually, useful long-distance quantum correlations can still be created if one performs the measurements depicted in Fig. 2b: half outcomes are used to gain information on  $T_o$ , and symmetrically for  $T_e$ , see Figs. 3 and 4.

As an example of the effect of the unknown syndromes in  $\mathcal{L}$ , let us consider that an error occurred on the center qubit  $A$ , and that all other qubits did not suffer any error. Since we do not know the syndromes of  $T_o$  that lie directly below and above  $T_X^*$ , we are not able to restore the  $X$  correlation. This occurs with probability  $p_X = p + \mathcal{O}(p^2)$ . From this fact, one finds that the final state

on  $A$  and  $B$  is a mixed state of the form

$$\rho_{AB} = F_X F_Z |\Phi^+\rangle\langle\Phi^+| + p_X F_Z |\Psi^+\rangle\langle\Psi^+| + F_X p_Z |\Phi^-\rangle\langle\Phi^-| + p_X p_Z |\Psi^-\rangle\langle\Psi^-|, \quad (9)$$

with  $F_X = 1 - p_X$  and  $F_Z = 1 - p_Z$ . This state is known to be distillable, and thus useful from a quantum information perspective, whenever its fidelity  $F_{AB} \equiv F_X F_Z$  is larger than one-half [22]. This can be achieved when the error rate  $p$  is smaller than a threshold  $p^*$ . In the next paragraphs, we first prove a lower bound on this value,  $p^* \gtrsim 1.17 \times 10^{-3}$ , and then present numerical results, showing that the real threshold is indeed much larger:  $p^* \gtrsim 2.27\%$ .

### 1. Correlation loss due to the missing syndromes in $T_o$

Paths of errors, which we generically denote by  $\Gamma$ , have a non-trivial effect on the  $X$  correlation if they cross the plane  $T_X^*$  an odd number of times, as depicted in Fig. 4. Moreover, the number  $l$  of errors which actually occur on a path  $\Gamma$  is at least  $L/2$ , where  $L$  denotes its length. This is the case because our error correction always leads to a minimum pairing of the syndromes  $s = -1$ . We now follow Chap. V in [21] to find an upper bound on the probability  $p_X$  of inferring the wrong quantum correlation:

$$p_X \leq 2 \sum_{\Gamma_{\mathcal{L}\mathcal{L}}} \text{prob}(\Gamma_{\mathcal{L}\mathcal{L}}) + \sum_{\Gamma_{\mathcal{L}\mathcal{R}}} \text{prob}(\Gamma_{\mathcal{L}\mathcal{R}}) + \sum_{\Gamma_{\mathcal{T}\mathcal{B}}} \text{prob}(\Gamma_{\mathcal{T}\mathcal{B}}) + 4 \sum_{\Gamma_{\mathcal{T}\mathcal{L}}} \text{prob}(\Gamma_{\mathcal{T}\mathcal{L}}), \quad (10)$$

where  $\mathcal{B}$  and  $\mathcal{T}$  stand for the bottom and top faces. Note that we already took into account the symmetries of the problem in this expression. For convenience, let us now introduce a new coordinate system  $(t_1, t_2, t_3)$  for the vertices of  $T_o$ , such that  $-N_o \leq t_1 \leq N_o$ ,  $-N_o < t_2 \leq N_o$ , and  $0 \leq t_3 \leq 2N_o$ , with  $N_o = (N-1)/4$ , see also Fig. 3. In this coordinate system, paths of errors  $\Gamma_{\mathcal{T}\mathcal{L}}$  travel a distance  $L \geq N_o$  and can start from  $N_o^2$  missing syndromes in  $T_o$  (lower triangle in  $\mathcal{L}$ ). Because for each vertex there are, in a cubic lattice, at most  $5^L/2$  self-avoiding walks pointing upward, we find that the last term of Eq. (10) is upper bounded by

$$\sum_{\Gamma_{\mathcal{T}\mathcal{L}}} \text{prob}(\Gamma_{\mathcal{T}\mathcal{L}}) \leq N_o^2 \sum_{L \geq N_o} \frac{5^L}{2} \sum_{l=\lceil L/2 \rceil}^L \binom{L}{l} p^l (1-p)^{L-l},$$

where  $\lceil L/2 \rceil$  denotes the smallest integer not less than  $L/2$ . The sum over  $l$ , together with the binomial coefficients, counts all possible paths of errors that appear in a given walk. One can check that the bound tends to 0 in the limit  $N_o \rightarrow \infty$  if  $10\sqrt{p(1-p)} < 1$ , i.e. if  $p \lesssim 1\%$ . The same result holds for the paths  $\Gamma_{\mathcal{L}\mathcal{R}}$  and  $\Gamma_{\mathcal{T}\mathcal{B}}$ ; note that this value is about three times smaller than the real critical point  $p_c \approx 3.3\%$ . Similar considerations for the

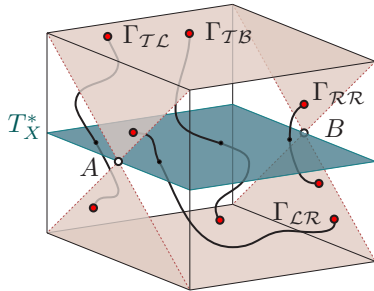


FIG. 4: (Color online) Some paths of errors that have a non-trivial effect on the long-distance entanglement: any path stretching from one shaded area to another, and crossing the plane  $T_X^*$  an odd number of times, degrades the  $X$  correlation between  $A$  and  $B$ . The shaded areas, which partially wrap the cube, are of two types: the top and bottom ones are the usual rough surfaces present in (three-dimensional) surface codes. The left and right shaded areas represent the unknown syndromes of  $T_o$ , see Fig. 3a. The situation for  $T_e$  is very similar (the picture is rotated by  $90^\circ$  around the  $AB$  axis), with the difference that all shaded areas are rough surfaces in this case.

paths  $\Gamma_{\mathcal{L}\mathcal{L}}$  finally yield, for  $p < 1\%$ ,

$$p_X \leq 2 \sum_{\Gamma_{\mathcal{L}\mathcal{L}}} \text{prob}(\Gamma_{\mathcal{L}\mathcal{L}}) \leq 2 \sum_{t_2 \geq 1} 2t_2 \sum_{L \geq t_2} \frac{5^{L-2}}{2} \sum_{l \geq \lceil L/2 \rceil} \binom{L}{l} p^l (1-p)^{L-l}. \quad (11)$$

This bound never tends to zero, but still converges if  $p$  is small enough. Before computing a threshold for  $F_{AB}$ , however, we first have to consider the errors made in the other sublattice.

## 2. Loss of correlation in $T_e$ and fidelity of the final state

The situation for the  $Z$  correlation is very similar to the previous case, since the measurement pattern is symmetric. Nonetheless there is a small difference: the missing syndromes do not lie on the vertices of the sublattice, but rather on its outer edges  $\mathcal{L}$  and  $\mathcal{R}$ . This creates additional parts of rough faces in  $T_e$ . It follows that the corresponding paths of errors have their first and last edges pointing in the  $t_3$  direction, so that a slightly better bound for the error  $p_Z$  can be derived:

$$p_Z \leq 2 \sum_{t_1 \geq 1} 2t_1 \sum_{L \geq t_1+2} \frac{5^{L-2}}{2} \sum_{l \geq \lceil L/2 \rceil} \binom{L}{l} p^l (1-p)^{L-l}. \quad (12)$$

Combining the two bounds on  $p_X$  and  $p_Z$  we find

$$p \lesssim 1.17 \times 10^{-3} \Rightarrow F_{AB} > 1/2, \quad (13)$$

which corresponds, via Eq. (4), to an error rate  $\varepsilon \lesssim 1.95 \times 10^{-4}$  in the initial connections. This value is quite small, mainly because our counting of paths of errors is very crude. Note that there are only few such paths of

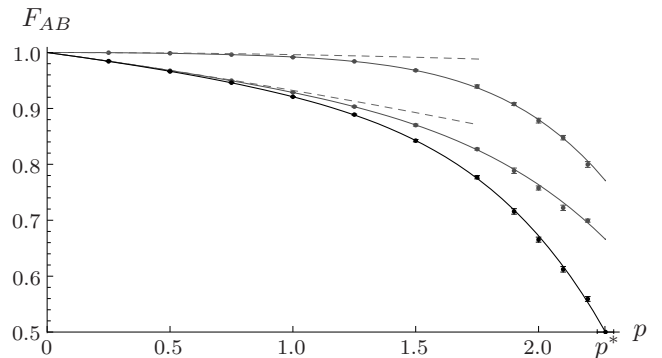


FIG. 5: Fidelity  $F_{AB} = F_X F_Z$  of the long-distance entangled state  $\rho_{AB}$  as a function of the error rate  $p$  (in percent). The critical value  $F^* = 0.5$  is reached at  $p^* = 2.27 \pm 0.03$  [%]. The upper curve represents the probability of success  $F_Z$  of the error correction in  $T_e$ , while the middle one is the function  $F_X$ . Corresponding series expansions for  $p \ll 1$  are plotted with dashed lines.

small length, and therefore this analytical bound could be increased by carefully computing its smallest orders in  $p$ . At this point, however, we prefer to turn to Monte Carlo simulations to find a much better estimate of the error threshold. We refer the reader to App. C for a description of the algorithm; in particular we propose an intuitive and efficient method, even if not optimal, to infer the value of the missing syndromes. The result of these simulations is plotted in Fig. 5: long-distance entanglement is achieved for error rates smaller than

$$p^* \approx 2.27\%, \quad (14)$$

i.e.  $\varepsilon^* \approx 3.86 \times 10^{-3}$  for the original lattice. Before concluding, let us comment on these thresholds:

- The values of the unknown syndromes are not optimally inferred in our algorithm, and therefore a higher value of  $p^*$  may be found. However, it is clear that it cannot exceed the critical error rate  $p_c \approx 3.3\%$ .
- One could get a higher threshold  $\varepsilon^*$  by directly computing  $F_{AB}$  as a function of  $\varepsilon$ . In fact, errors in the faces  $\mathcal{L}$  and  $\mathcal{R}$  do not appear with probability  $p \approx 6\varepsilon$ , but only with probability  $p \approx 5\varepsilon$ .
- Our measurement pattern puts  $T_o$  and  $T_e$  on the same footing (Figs. 2 and 3), but it could be profitable to get more information on the unknown syndromes of  $T_o$  since the  $X$  correlation is more sensitive to errors.
- Finally, as suggested in [17, Rem. 2], lattices of size  $\log(N) \times \log(N) \times N$  may also be appropriate for generating long-distance entanglement. This result also holds in our setting, because additional errors only appear in the faces  $\mathcal{L}$  and  $\mathcal{R}$  and not in the bulk of the lattice.

## V. CONCLUSION

We have investigated the problem of generating long-distance entanglement in noisy quantum networks. We have focused on three-dimensional regular lattices, whose edges are full-rank mixed states of two qubits. We have proven that entanglement can be established between two infinitely distant qubits if the fidelity of the connections is large enough. Our protocol starts by transforming the quantum network into a thermal cluster state. Then, all but two distant qubits are measured according to a specific pattern of local bases, and a syndrome-based error correction is performed. The error recovery is very similar to the one used for planar codes, with the difference being that our setting does not allow one to get complete information on the syndromes. Nevertheless, useful quantum correlations can be created between the two unmeasured qubits if the error rate is smaller than a critical value. We have given both an analytical lower bound on this value and a numerical estimation (about 2%) based on Monte Carlo simulations.

In conclusion, we have shown that a constant overhead of local resources is sufficient to achieve long-distance communication in quantum networks. This contrasts with previous one- or two-dimensional strategies, in which the physical resources per station increase with the distance. Our protocol requires perfect local quantum operations, which is somehow justified by the fact that most errors occur while sending quantum information between stations. It would nevertheless be of fundamental interest to design fault-tolerant protocols, in two or three dimensions, for which the overhead of local resources is as small as possible.

### Acknowledgments

The author thanks Ignacio Cirac and Antonio Acín for initiating the project and for useful discussions. This work has been supported by the QCCC program of the Elite Network of Bavaria.

### Appendix A: Elementary entangled pairs of qubits

We show in this appendix that there is no loss of generality in choosing the elementary links to be described by Eq. (1). First, it is well known that any two-qubit entangled state can be brought to the rotationally symmetric mixture

$$W_F = F |\Phi^+\rangle\langle\Phi^+| + \frac{1-F}{3} |\Psi^+\rangle\langle\Psi^+| + \frac{1-F}{3} |\Phi^-\rangle\langle\Phi^-| + \frac{1-F}{3} |\Psi^-\rangle\langle\Psi^-|. \quad (\text{A.1})$$

In fact, this is achieved by applying random bilateral rotations, locally, to each qubit. This state is called a

Werner state [23] and has the same fidelity  $F$  as the initial state from which it derives. Let us denote  $W_F$  by its components in the Bell basis,  $W_F = (F, \frac{1-F}{3}, \frac{1-F}{3}, \frac{1-F}{3})$ , and define the two unitaries

$$H = \frac{1}{\sqrt{2}} \begin{pmatrix} 1 & 1 \\ 1 & -1 \end{pmatrix} \quad \text{and} \quad H' = \frac{1}{\sqrt{2}} \begin{pmatrix} i & 1 \\ 1 & i \end{pmatrix}. \quad (\text{A.2})$$

One can check that the separable operation  $H \otimes H$  applied on a Bell-diagonal state switches its coefficients  $\Phi^-$  and  $\Psi^+$ , while the coefficients  $\Phi^+$  and  $\Psi^-$  are unaltered. A similar result holds for  $H' \otimes H'$ , which only switches the components  $\Phi^+$  and  $\Psi^+$ . Suppose now that an entangled pair  $W_F$ , with  $F = 1 - 3\varepsilon^2$ , has been created between two neighboring nodes. This already sets the coefficient  $\Psi^-$  to the desired value  $\varepsilon^2$ . Then, apply  $H' \otimes H'$  with probability  $p = \frac{2\varepsilon}{1+2\varepsilon}$ , and  $\mathbb{1} \otimes \mathbb{1}$  with probability  $1 - p$  on  $W_F$ . This leads to the state  $((1-\varepsilon)^2, \varepsilon(2-3\varepsilon), \varepsilon^2, \varepsilon^2)$ . Finally, repeat the operation by applying  $H \otimes H$  with probability one-half. Both coefficients  $\Psi^+$  and  $\Phi^-$  are set to  $\varepsilon(1-\varepsilon)$ , which proves that the state  $\rho$  given in Eq. (1) is indeed general.

### Appendix B: Basics of syndrome-based error correction

Let us consider the sublattices  $T_o$  and  $T_e$  described in the text, in which  $Z$  errors occur independently on each edge with probability  $p$ , and assign to each vertex the syndrome  $s = +1$  if it is connected to an even number of erroneous edges, and  $s = -1$  otherwise. In the case of perfect and complete syndrome information, one knows exactly where all paths of errors start and end: this occurs at syndromes  $s = -1$ . In the regime of small error rate  $p$ , it turns out that the best error recovery strategy is to pair these syndromes such that the total length of all pairings is minimized. Then, one connects any two paired syndromes by a path of minimum length, and artificially introduces  $Z$  “errors” along these paths. This creates loops of errors in the cluster state, which, however, do not cause any damage to the long-distance quantum correlations. In fact these loops either do not intersect the planes  $T_X^*$  and  $T_Z^*$  or cross them twice, and consequently do not modify the eigenvalues in Eq. (6).

Problems arise because some syndromes are unknown. For instance, consider the edges that have only one extremity in  $V(T_o)$  or  $V(T_e)$ : their coordinates are  $(o, 0, o)$  and  $(o, N-1, o)$  in  $T_o$ , and  $(1, e, e)$  and  $(N, e, e)$  in  $T_e$ , see Fig. 3. These are the rough faces described in [17], and errors on these edges change the sign of only one syndrome (and not two) in the corresponding sublattice. An equivalent viewpoint is that both extremities of these edges indeed belong to  $T_o$  or  $T_e$ , but we do not have access to their outer syndrome. The consequence of this lack of information is that some paths of errors  $\Gamma$  are not closed anymore, but rather originate from a missing syndrome and terminate at another. Typically, these open paths enter only superficially the lattice if the error rate  $p$  is small, but they start stretching from one side

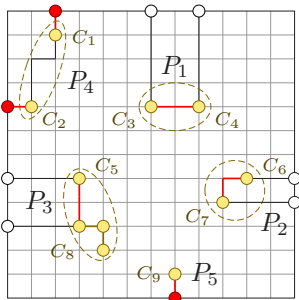


FIG. 6: (Color online) An example of how unknown syndromes, which here lie on the boundary, are assigned the value  $\pm 1$ . We first find all odd-size clusters  $C_i$  of syndromes  $-1$ , which are drawn in light yellow (light gray), and pair them by increasing distance. A cluster may be left alone; in that case we add it in the end of the sorted list of cluster pairs  $P_i$ . Then, for each  $P_i$ , we check if it is favorable to add two new syndromes  $-1$ . Here, this is the case only for  $P_4$  and  $P_5$ .

to another as soon as  $p$  exceeds the value  $p_c \approx 3.3\%$ . In the latter case, paths of errors can cross an odd number of times the planes of correlations, which results in a complete loss of long-distance entanglement in the limit  $N \rightarrow \infty$ .

### Appendix C: Monte Carlo simulations

We now describe the algorithm used for computing the data of Fig. 5. The correction procedure is very similar for the two sublattices  $T_o$  and  $T_e$ , and consists of two main parts. First, given a lattice with random errors, we infer the value of the syndromes for which we have no information. Second, we proceed with the usual error recovery. The program outputs 1 if the correction is successful, and 0 otherwise.

#### a. Inferring the missing syndromes

We propose a very simple way of assigning the value  $+1$  or  $-1$  to the missing syndromes, so that a good approximation of the optimal configuration is found. To that end, it is helpful to consider a typical realization of a noisy cluster state in the regime of small error rates, as depicted in Fig. 6. Our algorithm reads

- Initialize all unknown syndromes to  $+1$ .
- Using nearest-neighbor site percolation, find all clusters  $C_i$  of syndromes  $-1$ . Keep only the clusters of odd size, and for each compute the minimum distance  $d_i$  to a closest unknown syndrome  $s_i$ . [26] Let  $n$  denote the number of such clusters. Note that we do not consider clusters of even size, since good pairings can be found for them, individually.

- Calculate the distance  $d_{ij}$  between all pairs of clusters  $C_i$  and  $C_j$ . This distance could be the length of the shortest path from  $C_i$  to  $C_j$ , but in practice it is much easier to calculate the distance between their “centers of mass.”
- Find  $C_a$  and  $C_b$  such that  $d_{ab} = \min\{d_{ij}\}$ , and create a pair  $P_1 = \{C_a, C_b\}$ . Remove  $C_a$  and  $C_b$  from the list of clusters, and repeat the procedure until no cluster is left. In case of odd  $n$ , add an extra “pair”  $\{C_i, C_i\}$  for the remain cluster, with  $d_{ii} = \infty$ . This creates the list  $\{P_1, \dots, P_{n/2}\}$ .
- For each  $P_k = \{C_i, C_j\}$ , check if  $d_{ij} > d_i + d_j$ . If this inequality holds, inverse the value of the corresponding missing syndromes:  $s_i \leftarrow (-s_i)$  and  $s_j \leftarrow (-s_j)$ .

The proposed algorithm is optimal in the regime of very dilute errors, but this is not true for high error rates anymore (even if results are good for all  $p$ ). Note that there exist optimal algorithms which are based on minimal perfect matchings in weighted graphs and are run in a polynomial time (see [24], Chap. 4). For three-dimensional lattices, however, the number of edges in these graphs scales as  $\mathcal{O}(N^6)$  [they are nearly complete graphs on  $\mathcal{O}(N^3)$  vertices], and therefore these algorithms are not so efficient in practice. Nevertheless, it would be very interesting to implement an optimal algorithm and decide whether the unknown syndromes are responsible for the threshold, or whether the equality  $p^* = p_c$  holds.

#### b. Error recovery

We use the well-known and efficient algorithm described by J. Edmonds in [25] to find an optimal pairing of the syndromes  $-1$ . The error correction is successful if the parity of paths of errors crossing the plane of correlation is even. Simulations of the error corrections have been performed for various lattice sizes (up to  $\approx 15^3$  nodes), and for both  $X$  and  $Z$  correlations. The extrapolation to infinite lattices is done by fitting the data with an exponential function, see Fig. 7. Results are plotted in Fig. 5.

Finally, let us present evidence that our algorithm gives correct and optimal results in the regime of small error rates. Considering the series expansions of  $p_X$  at first order in  $p$ , one sees that only three edges of  $\mathcal{L}$  may degrade the  $X$  correlation: these are the bonds in  $T_o$  that cross  $T_X^*$  and whose first coordinate  $t_1$  belongs to  $\{-1, 0, 1\}$ , see Fig. 3a. At second order, one can check that the probability to infer the wrong  $X$  correlation due to the missing syndromes in  $\mathcal{L}$  is  $p_X^L = 3p + 48p^2$ . Therefore, by symmetry, the fidelity  $F_X = 1 - p_X^L(1 - p_X^R) - p_X^R(1 - p_X^L)$  reads

$$F_X = 1 - 6p - 78p^2 + \mathcal{O}(p^3). \quad (\text{C.1})$$

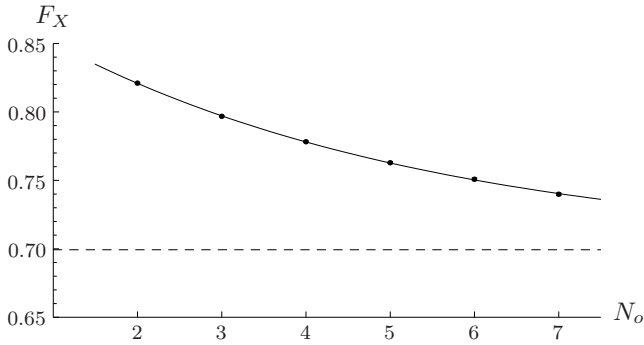


FIG. 7: Fidelity  $F_X$  in the limit  $N_o \rightarrow \infty$ , for a fixed error rate  $p$ . We use the function  $F_X^{(\infty)} + a e^{-b N_o}$  to fit the data computed from lattices consisting of  $(2N_o+1) \times (2N_o) \times (2N_o+1)$  nodes. At least  $10^5$  simulations have been run for each value of  $N_o \in \{2, 3, \dots, 7\}$ . In this example the error rate is  $p = 2.2\%$ , and the fit yields  $F_X^{(\infty)} = 0.699 \pm 0.003$ .

It is easy to see that a single error in  $T_e$  cannot damage the  $Z$  correlation, and a careful counting of configurations with two errors yields  $p_Z^2 = 19p^2$ . Consequently we find

$$F_Z = 1 - 38p^2 + \mathcal{O}(p^3). \quad (\text{C.2})$$

These two series expansions are plotted (dashed lines) in Fig. 5: they agree perfectly with the results of the Monte Carlo simulations and thus validate our algorithm.

- 
- [1] H. J. Kimble, *Nature* **453**, 1023 (2008).
- [2] J. I. Cirac, A. K. Ekert, S. F. Huelga, and C. Macchiavello, *Phys. Rev. A* **59**, 4249 (1999).
- [3] C. H. Bennett, G. Brassard, C. Crepeau, R. Jozsa, A. Peres, and W. K. Wootters, *Phys. Rev. Lett.* **70**, 1895 (1993).
- [4] W. Dür, H.-J. Briegel, J. I. Cirac, and P. Zoller, *Phys. Rev. A* **59**, 169 (1999).
- [5] L.-M. Duan, M. D. Lukin, J. I. Cirac, and P. Zoller, *Nature* **414**, 413 (2001).
- [6] L. Hartmann, B. Kraus, H.-J. Briegel, and W. Dür, *Phys. Rev. A* **75**, 032310 (2007).
- [7] L. I. Childress, J. M. Taylor, A. S. Sørensen, and M. D. Lukin, *Phys. Rev. A* **72**, 052330 (2005).
- [8] N. Sangouard, C. Simon, H. de Riedmatten, and N. Gisin, eprint arXiv:quant-ph/0906.2699.
- [9] L. Jiang, J. M. Taylor, K. Nemoto, W. J. Munro, R. V. Meter, and M. D. Lukin, *Phys. Rev. A* **79**, 032325 (2009).
- [10] A. Acín, J. I. Cirac, and M. Lewenstein, *Nature Phys.* **3**, 256 (2007).
- [11] S. Perseguers, L. Jiang, N. Schuch, F. Verstraete, M. Lukin, J. Cirac, and K. Vollbrecht, *Phys. Rev. A* **78**, 062324 (2008).
- [12] A. G. Fowler, D. S. Wang, T. D. Ladd, R. V. Meter, and L. C. L. Hollenberg, eprint arXiv:quant-ph/0910.4074.
- [13] G. K. Brennen, C. M. Caves, P. S. Jessen, and I. H. Deutsch, *Phys. Rev. Lett.* **82**, 1060 (1999).
- [14] R. Ionicioiu and W. J. Munro, eprint arXiv:quant-ph/0906.1727.
- [15] R. Raussendorf and J. Harrington, *Phys. Rev. Lett.* **98**, 190504 (2007).
- [16] S. Broadfoot, U. Dorner, and D. Jaksch, *EuroPhys. Lett.* **88**, 50002 (2009).
- [17] R. Raussendorf, S. Bravyi, and J. Harrington, *Phys. Rev. A* **71**, 062313 (2005).
- [18] M. Hein, W. Dr, R. Raussendorf, M. V. den Nest, and H.-J. Briegel, in *Quantum Computer, Algorithms and Chaos* (IOS, Amsterdam, 2006), vol. 162 of *International School of Physics Enrico Fermi*, edited by G. Casati, D. L. Shepelyansky, P. Zoller, and G. Benenti.
- [19] F. Verstraete and J. I. Cirac, *Phys. Rev. A* **70**, 060302(R) (2004).
- [20] T. Ohno, G. Arakawa, I. Ichinose, and T. Matsui, *Nucl. Phys.* **B697**, 462 (2004).
- [21] E. Dennis, A. Kitaev, A. Landahl, and J. Preskill, *J. Math. Phys.* **43**, 4452 (2002).
- [22] D. Deutsch, A. Ekert, R. Jozsa, C. Macchiavello, S. Popescu, and A. Sanpera, *Phys. Rev. Lett.* **77**, 2818 (1996).
- [23] R. F. Werner, *Phys. Rev. A* **40**, 4277 (1989).
- [24] D. S. Wang, A. G. Fowler, A. M. Stephens, and L. C. L. Hollenberg, eprint arXiv:quant-ph/0905.0531.
- [25] J. Edmonds, *Canad. J. Math.* **17**, 449 (1965).
- [26] Several such syndromes may exist; choose the one that lie in the plane parallel to  $T_X^*$  or  $T_Z^*$  that contains  $C_i$ . This avoids unnecessary crossings of the plane of correlation.